Excitations of pygmy dipole resonances in exotic and stable nuclei via Coulomb and nuclear fields

E. G. Lanza,[1,2] A. Vitturi,[3,4] M. V. Andrés,[5] F. Catara,[2,1] and D. Gambacurta[2,1]
[1]*INFN Sezione di Catania, Catania, Italy*
[2]*Dipartimento di Fisica e Astronomia, Universitá di Catania, Catania, Italy*
[3]*Dipartimento di Fisica, Universitá di Padova, Italy*
[4]*INFN Sezione di Padova, Padova, Italy*
[5]*Departamento de FAMN, Facultad de Física, Sevilla, Spain*
(Received 25 July 2011; published 2 December 2011)

We study heavy-ion inelastic scattering processes in neutron-rich nuclei including the full response to the different multipolarities. Among these we focus in particular on the excitation of low-lying dipole states commonly associated to the pygmy dipole resonance. The multipole response is described within the Hartree-Fock plus RPA formalism with Skyrme interaction. We show how the combined information from reactions processes involving the Coulomb and different mixtures of isoscalar and isovector nuclear interactions can provide a clue to reveal the characteristic features of these states. We have performed calculation for the excitation of ^{132}Sn generated in the reactions with ^{4}He, ^{40}Ca, and ^{48}Ca at several incident energies, as well as for the system ^{17}O + ^{208}Pb. Our results suggest that the investigation of the PDR states can be better carried out at low incident energies (below 50 MeV/nucleon). In fact, at these energies the PDR peak is relatively stronger than the giant dipole resonance (GDR) one and the narrow width of the low-lying quadrupole and octupole states should not blur its presence.

DOI: 10.1103/PhysRevC.84.064602 PACS number(s): 24.30.Gd, 21.60.Jz, 25.60.−t, 25.70.−z

I. INTRODUCTION

In the last years the properties of collective states in neutron-rich nuclei have been studied with special attention to the presence of dipole strength at low excitation energy [1]. Previous calculations [2] have shown that as soon as the neutron number increases, some strength appears at low energies in the dipole strength distribution, well below the dipole giant resonance. This strength, carrying few percent of the isovector EWSR, is present in many isotopes and has been often associated to the possible existence of a new collective mode of new nature: the pygmy dipole resonance (PDR).

These low-lying dipole modes have been studied and are known since many years. To our knowledge it was Lane [3] who first named them after the tiny strength of the state as compared to the giant dipole resonance (GDR) one. At the same time, macroscopic approaches were developed like the incompressible three fluid model [4] (proton, neutron of the core, and the neutron excess) on the same spirit of the Steinwedel-Jensen model [5]. Within this model the existence of the low-lying dipole state is found in a natural way, although the calculated strength of the PDR was too weak. An improved version of the model is given in Ref. [6] where only two incompressible fluids were considered, namely the core and the neutron excess. The so generated pygmy resonances have a strength in reasonable agreement with the experimental data available at that time [7], for some β stable nuclei having few neutron excess. Another macroscopic approach that takes explicitly into account the neutron skin [8] follows the Goldhaber-Teller prescription [9], finding that the ratio of the PDR to the GDR sum rule is similar to the one obtained in Ref. [6]. Recently, a macroscopic model where the nucleus is considered as a spherical piece of elastic continuous medium [10] has investigated the PDR in terms of elastodynamics excitation mechanism implying then the isoscalar nature of the state.

These low-lying dipole modes have been extensively studied within several microscopic many-body models [1] among which we quote the Hartree-Fock plus random phase approximation (RPA) with Skyrme interactions or quasiparticle RPA [11]; the relativistic RPA (RRPA) [12]; and the relativistic Hartree Bogoliubov (RHB) plus the relativistic quasiparticle RPA (RQRPA) [13]; the RRPA plus phonon coupling (PC) [14]; the QRPA plus the quasiparticle phonon coupling (QPM) [15]. This is by no means an exhaustive list of the literature devoted to this subject. Here we quote the more significant references in order to provide to the interested reader a first hint on the exploration of the entire subject. All these approaches predict the presence of the low-lying states with similar strengths and similar transition densities. Whether such strength corresponds (or not) to a collective mode is still under discussion. Several authors have taken as measure of the collectivity the number of particle-hole configurations entering in the RPA wave function with an appreciable weight [12,16]. Such criteria do not take into account the other fundamental concept that underlies collectivity, that is coherence. Indeed, in Ref. [17] we conclude that although the PDR are formed by many particle hole configurations their collective nature may be questioned if one takes into account also the coherence properties.

Experimental information for these states have come from high-energy Coulomb excitation processes with heavy ion collisions produced at GSI on ^{132}Sn [18,19] as well as on ^{68}Ni [20]. They have clearly shown the presence of these states. Another well-established method to study the PDR is by means of nuclear resonance fluorescence (or real photon-scattering experiments) performed on semimagic nuclei at Darmstadt [21]. Recently, the same nuclei have been investigated by means of the $(\alpha, \alpha'\gamma)$ coincidence method at KVI [22].

The experimental investigation, corroborated by theoretical studies, clearly show that the PDR modes are connected to the

 ©2011 American Physical Society

neutron excess. The strength of the PDR has been related to the neutron skins and to the density dependence of the symmetry energy of nuclear matter [19,23]. In particular, recent studies have also put a constraint to the kind of Skyrme force one has to use in the mean field + RPA-like calculations [24]. One should note, however, that the occurrence of different radii for the proton and neutron densities and the consequent low-lying strength also appears in neutron-rich stable nuclei.

Therefore a deeper knowledge of the properties of the PDR is in order. But, as stated above, until now the evidence for these states comes essentially from heavy-ion induced Coulomb excitation processes which provide information only on the $B(E\lambda)$ transition rates. In order to understand better the nature of these states one has to obtain more explicit information also on wave functions and transition densities. To this end one can envisage different reactions where the nuclear part of the interaction is involved. Indeed, due to the mixed nature displayed by these states it is possible to excite them also with an isoscalar probe like the one provided by the nuclear part of the interaction. In this paper we will show how the excitation probabilities are sensitive to the details of the transition densities and the corresponding form factors and how these can be probed by combination of different processes. Indeed, by choosing, in an appropriate way, the projectile mass, charge, bombarding energy, and scattering angle, the relative role of the nuclear and Coulomb components can be modified, as well as the relative population of the different multipolarities and the relative importance of the low-lying and high-lying parts of the response. Therefore a proper choice of the reaction parameters can produce an enhancement of the PDR population.

II. RPA DIPOLE STRENGTH DISTRIBUTION

The presence of low-lying strength in neutron-rich nuclei is predicted by almost all theoretical models. We will show and discuss the microscopic results obtained in the simplest discrete nonrelativistic RPA approach with Skyrme interactions. We have performed calculations for several Sn isotopes [17]. To better appreciate the isotope dependence, three distributions of dipole strength are shown together in the upper part (a) of Fig. 1. The discrete RPA results are folded with Lorentzians of 1 MeV width to produce the smoothed curves plotted in the figures. As soon as we increase the mass number an increasing amount of low-lying strength (carrying a fraction of the EWSR of the order of few percent) below 10 MeV appears. These are precisely the states that are candidates to be interpreted as pygmy dipole resonances: they are generally associated with the occurrence of neutron skins in the nuclear densities. Actually, the presence of the low-lying dipole strength is not a prerogative of exotic nuclei but it is also present in stable nuclei with neutron excess as it is the case for ^{208}Pb, whose dipole strength distribution is shown in the lower part (b) of Fig. 1. In the same frame we plot the discrete RPA results as well as the smoothed curve. Indeed, in the figure one can appreciate the presence of a small bump around 7.9 MeV whose strength is about 1.1% of the EWSR. This state, as it is shown below, has the same characteristic feature of the PDR. We note that in ^{208}Pb the neutron and proton root mean square radii are 5.59 and 5.45 fm, respectively, while in ^{132}Sn they are 4.86 and 4.66 fm.

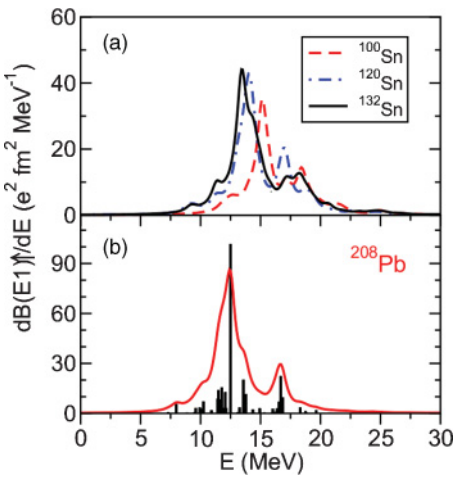

FIG. 1. (Color online) Isovector strength distributions for dipole states for tin isotopes calculated with the SGII interaction (upper frame). In the lower frame, the bars represent the results for the discrete RPA dipole strength. In this case the $B(E1)$'s are in units of (e^2fm^2). The solid curves are obtained by adopting a smoothing procedure as described in the text.

Precise information on the specific nature of the states is contained in their transition densities. As an example, in Fig. 2 we show the RPA transition densities for the low-lying dipole states in two cases: ^{208}Pb (lower frame) and ^{132}Sn (upper frame). They were calculated with the SGII interaction [25]. The neutron (dot-dashed) and proton (dashed) components of the transition densities oscillate in phase in the interior region, while in the external region only the neutrons give a contribution to both isoscalar and isovector transition densities which have the same magnitude. Such behavior, which has been found also in all the other microscopic approaches, can be taken as a sort of definition of PDR. The transition densities of the two nuclei are very similar. The main difference manifests in the isovector part which in the case of ^{208}Pb has one more node with respect to the ^{132}Sn one. This may be simply related to the different active major shells in the two nuclei and may be a further manifestation of the non collective character of the PDR states. Both of them show a strong isospin mixing in the peripheral region of the transition density. This feature opens the possibility to populate these states also via an isoscalar probe [26]. Therefore we will investigate this new mode with the help of a semiclassical model where the excitation processes will be carried out by both nuclear and Coulomb interactions.

In Ref. [17] these low-lying dipole states have been extensively analyzed questioning their collective nature. Also, the usual macroscopic interpretation of the neutron skin oscillating against the proton + neutron core has been discussed and put in doubt [27]. A simple macroscopic description of such model yields transition densities which are similar to the microscopic ones but not enough to give a conclusive interpretation of the state in terms of the above macroscopic model. It should be noted that, besides the requirement of the shape of the transition density, the macroscopic picture should also involve

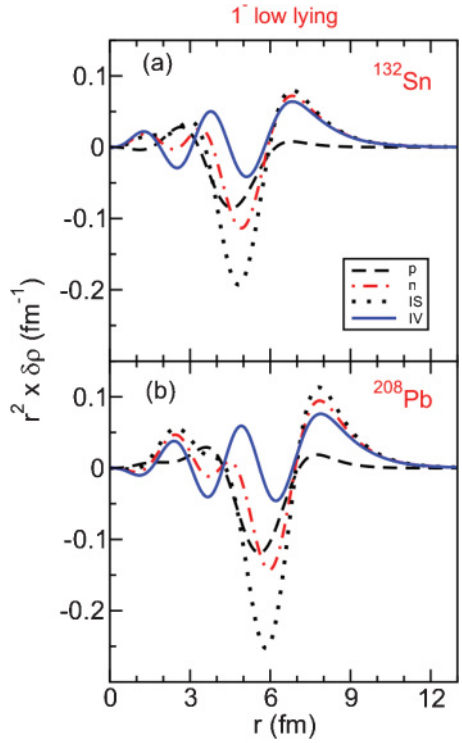

FIG. 2. (Color online) RPA transition densities for the low-lying dipole states for ^{208}Pb (lower frame) and ^{132}Sn (upper frame) calculated with the SGII interaction. As indicated in the legend we plot the proton, neutron, isoscalar and isovector components

a collective nature of the state, which was not found to be fulfilled at least in our calculations [17].

III. SEMICLASSICAL MODEL AND FORM FACTORS

The reaction processes are described according to the semiclassical model which assumes that the colliding nuclei move on classical trajectories, while the internal degrees of freedom are treated quantum mechanically. This model is known to hold for heavy-ion grazing collisions. We will consider, for simplicity, only target excitations. Therefore, under these conditions, we can write the Hamiltonian as

$$H_T = H_T^0 + W(t), \tag{1}$$

where H_T^0 is the internal hamiltonian of the target and the external field W describes the excitation of T by the mean field U_P of the partner nucleus, whose matrix elements depend on time through the relative coordinate $\mathbf{R}$(t):

$$W(t) = \sum_{ij} \langle i|U_P(\mathbf{R}(t))|j\rangle a_i^\dagger a_j + \text{H.c.} \tag{2}$$

The sums over the single particle states, denoted by i and j, run over both particle and hole states. Calling $|\Phi_\alpha\rangle$ the eigenstates of the internal Hamiltonian, the cross section can be calculated, nonperturbatively, by solving the Schrödinger equation in the space spanned by the $|\Phi_\alpha\rangle$ states. Then the time dependent state, $|\Psi(t)\rangle$, of the target nucleus can be expressed as

$$|\Psi(t)\rangle = \sum_\alpha A_\alpha(t) e^{-iE_\alpha t}|\Phi_\alpha\rangle, \tag{3}$$

where the ground state is also included in the sum as the term $\alpha = 0$. The Schrödinger equation can be cast into a set of linear differential equations

$$\dot{A}_\alpha(t) = -i \sum_{\alpha'} e^{i(E_\alpha - E_{\alpha'})t} \langle \Phi_\alpha|W(t)|\Phi_{\alpha'}\rangle A_{\alpha'}(t) \tag{4}$$

whose solutions, the amplitudes $A_\alpha(t)$, are then used to construct the probability of exciting the internal state $|\Phi_\alpha\rangle$ as

$$P_\alpha(b) = |A_\alpha(t = +\infty)|^2 \tag{5}$$

for each impact parameter b. Finally, by integrating P_α over the impact parameters we obtain the cross section

$$\sigma_\alpha = 2\pi \int_0^{+\infty} P_\alpha(b) T(b) b db. \tag{6}$$

The transmission coefficient $T(b)$ takes into account processes not explicitly included in the model space. It is usually taken as a depletion factor that falls to zero as the overlap between the two nuclei increases. A standard practice is to construct it from an integral along the classical trajectory as

$$T(b) = \exp\left\{-\frac{2}{\hbar}\int_{-\infty}^{+\infty} V_I(R(t'))dt'\right\}, \tag{7}$$

where V_I is the imaginary part of the optical potential associated to the studied reaction. When the imaginary part is not available from the experimental data we use the simple assumption of taking it as half of the real part.

The internal structure of the colliding nuclei is provided by the RPA approach. To reduce the complexity of the problem we include in the coupled-channel calculation only the states with a sizable EWSR percentage. In order to further reduce their number, we bunch together states with significant strength close in energy. The "bunching" procedure consists in taking as energy the average energy of the states belonging to the group with the condition that the EWSR must be preserved [17]. As an example in Table I are shown the dipole states obtained applying this procedure for ^{132}Sn.

The real part of the optical potential, which together with the Coulomb interaction determines the classical trajectory, is constructed with the double folding procedure [28,29]. Taking also the isospin dependent part of the nucleon-nucleon interaction and following the notation of Satchler's book [29] we write the central part of the local effective interaction v_{12} as composed by two terms, the isoscalar part v_0 generating

TABLE I. Dipole states used in the calculations.

States	E (MeV)	EWSR %
1^-_{ll} (PDR)	9.3	1.1
1^-_{ll2}	11.3	4.4
GDR	13.9	56
1^-_{hl}	18.3	25

an isoscalar ion-ion potential and an isovector term v_1 giving an isospin dependent folding potential which has an explicit dependence on the difference between the neutron and proton densities:

$$v_{12} = v_0(r_{12}) + v_1(r_{12})\tau_1 \cdot \tau_2, \tag{8}$$

where the τ_i's are the isospin of the nucleons. This implies that the neutron-neutron, proton-proton and neutron-proton interaction will be

$$v_{nn} = v_{pp} = v_0 + v_1, \; v_{np} = v_0 - v_1. \tag{9}$$

Then for the double folding we have

$$\begin{aligned} U_F &= \int\int \rho_P(r_1)\rho_T(r_2)v_{12}d\mathbf{r_1}d\mathbf{r_2} \\ &= \int\int [\rho_{Pn}(r_1)\rho_{Tn}(r_2)] + [\rho_{Pp}(r_1)\rho_{Tp}(r_2)] \\ &\quad \times(v_0 + v_1)d\mathbf{r_1}d\mathbf{r_2} \\ &\quad + \int\int [\rho_{Pn}(r_1)\rho_{Tp}(r_2)] + [\rho_{Pp}(r_1)\rho_{Tn}(r_2)] \\ &\quad \times(v_0 - v_1)d\mathbf{r_1}d\mathbf{r_2}, \end{aligned} \tag{10}$$

hence

$$U_{F_0} = \int\int \rho_P(r_1)\rho_T(r_2)v_0(r_{12})d\mathbf{r_1}d\mathbf{r_2}, \tag{11}$$

$$\begin{aligned} U_{F_1} &= \int\int \{\rho_{Pn}(r_1) - \rho_{Pp}(r_1)\} \\ &\quad \times\{\rho_{Tn}(r_2) - \rho_{Tp}(r_2)\}v_1(r_{12})d\mathbf{r_1}d\mathbf{r_2}. \end{aligned} \tag{12}$$

Note that in the particular case when $\rho_n = \rho_p(N/Z) = \rho(N/A)$ the last expression reduces to

$$\begin{aligned} U_{F_1} &= \left(\frac{N_T - Z_T}{A_T}\right)\left(\frac{N_P - Z_P}{A_P}\right) \\ &\quad \times \int\int \rho_P(r_1)\rho_T(r_1)v_1(r_{12})d\mathbf{r_1}d\mathbf{r_2}. \end{aligned} \tag{13}$$

For v_0 and v_1 we use the M3Y nucleon-nucleon interaction, Reid type [30], whose explicit expressions are [28]

$$v_0(r) = \left[7999\frac{e^{-4r}}{4r} - 2134\frac{e^{-2.5r}}{2.5r}\right] - 262\delta(\mathbf{r}) \tag{14}$$

and

$$v_1(r) = -\left[4886\frac{e^{-4r}}{4r} - 1176\frac{e^{-2.5r}}{2.5r}\right] + 217\delta(\mathbf{r}), \tag{15}$$

in MeV when r is given in fm. In the two above expressions the zero range term is the pseudopotential which takes into account, in an effective way, the single nucleon exchange [28].

The transition densities are the basic ingredients to construct the nuclear form factors describing nuclear excitation processes. These form factors can again be obtained by double folding [28,29] the transition densities with the density of the reaction partner and the nucleon nucleon interaction, including again both isoscalar and isovector terms. If one proceeds as in the case of the real part of the potential then the following

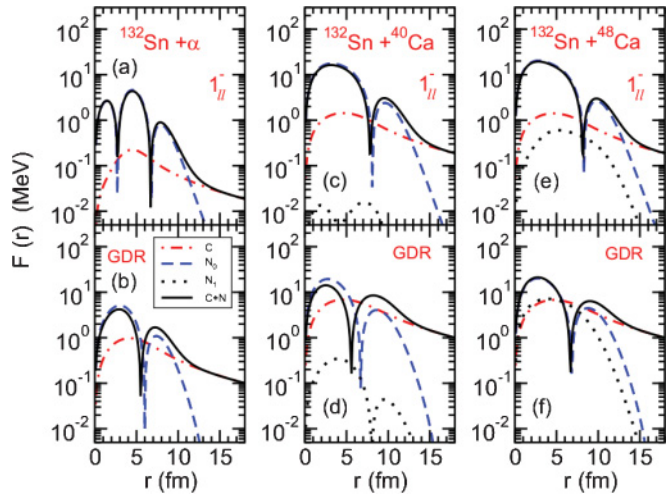

FIG. 3. (Color online) Form factors for three different systems ^{132}Sn + α, ^{40}Ca, ^{48}Ca. The upper parts refer to the PDR states while the lower ones are for the GDR. The different components are shown together with the total one (solid black line).

expressions for the form factors are obtained:

$$\begin{aligned} F_0 &= \int\int [\delta\rho_{Pn}(r_1) + \delta\rho_{Pp}(r_1)] \\ &\quad \times v_0(r_{12})[\rho_{Tp}(r_2) + \rho_{Tn}(r_2)]r_1^2dr_1r_2^2dr_2, \end{aligned} \tag{16}$$

$$\begin{aligned} F_1 &= \int\int [\delta\rho_{Pn}(r_1) - \delta\rho_{Pp}(r_1)] \\ &\quad \times v_1(r_{12})[\rho_{Tn}(r_2) - \rho_{Tp}(r_2)]r_1^2dr_1r_2^2dr_2. \end{aligned} \tag{17}$$

These two components of the form factor are indicated in Fig. 3 as N_0 and N_1, respectively.

IV. INELASTIC CROSS SECTION

A. The ^{132}Sn case

As a first example, we will consider the excitation of dipole states in ^{132}Sn by different partners: α, ^{40}Ca, and ^{48}Ca. The form factors for the PDR (upper frames) and GDR (lower frames) states are shown in Fig. 3. The Coulomb form factors (dashed dotted line) are almost one order of magnitude smaller for the PDR with respect to the GDR ones, as expected, from their relative $B(E1)$ strengths. On the other hand, the nuclear components have almost the same magnitude, hence their relative contribution in the excitation processes is stronger for the PDR states. The different isospin components are indicated with dashed line (the isoscalar part) and dotted line (isovectorial part). We get strong contribution from the isovector part only for the ^{48}Ca case while for α and ^{40}Ca the contribution is inhibited because of their pure isoscalar nature.

The nuclear and Coulomb parts interfere destructively at small radii and constructively at large radii. This is mainly due to isoscalar part and to the fact that the isoscalar dipole transition density displays nodes [2,31]. The interference is less pronounced in the ^{48}Ca case because of the presence of the isospin dependent part of the nuclear form factor that

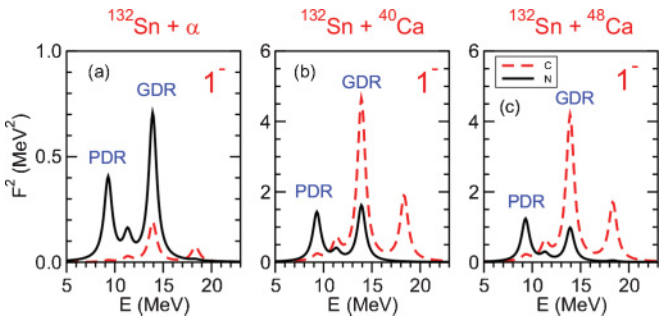

FIG. 4. (Color online) Square of the form factor for different systems ^{132}Sn + (α, ^{40}Ca, ^{48}Ca) as function of the energies. They are calculated at a distance where the transmission coefficients take the value of 0.5, namely 7.7 fm, 11.0 fm, and 11.3 fm for the three cases. Coulomb and nuclear contributions to the total form factors are separately shown. The same folding procedure used in Fig. 1 has been applied also in this case. Note the different ordinate scale in the left panel.

gives a contribution opposite to the Coulomb one without changing its sign. As a consequence, we expect that the excitation of the GDR state will be less pronounced when the ^{48}Ca is used as a target rather than ^{40}Ca. Conversely, one is not expecting significant change for the PDR state where the nuclear contribution is dominated by the isoscalar part. Indeed, this can be verified in a simple way by taking the square of the nuclear and Coulomb form factors at the surface. In Fig. 4 they are reported as a function of the excitation energy for the dipole states given in Table I. So, without taking into account the dynamics of the reactions, one can already at this stage anticipate how different projectiles will alter the relative intensities of the PDR and GDR states due to the different interplay of their isoscalar and isovector contributions. The above discussed properties are general enough and the use of a different nucleon-nucleon effective interaction should not change qualitatively the characteristic features of the form factors.

The ratios between PDR and GDR cross section can be modified by looking at the differential angular distributions. In the semiclassical picture, these are associated to different ranges of impact parameters. Nuclear contributions are known to be enhanced at grazing angles, corresponding to grazing impact parameters. This is clearly evidenced in Fig. 5, where the "partial-wave cross sections" are shown as functions of the impact parameter. We note that in all systems treated, at grazing impact parameters, the Coulomb contribution for the PDR is relatively smaller than the nuclear one. A different behavior is seen for the GDR case except for the α particles where the Coulomb excitation plays a less important role for both PDR and GDR.

The energy differential total cross sections for the dipole states are shown in Fig. 6 for the three cases considered at 30 MeV/nucleon incident energy. The discrete total cross sections obtained with Eq. (6) are smoothed out by folding them with Lorentzians whose widths depend on the energies. Rather than using the crude prescription adopted by ourselves in Ref. [17], we preferred to assign to the widths a smooth

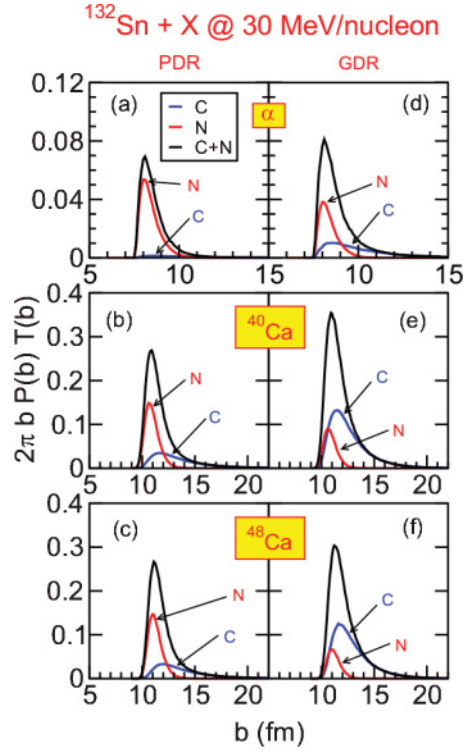

FIG. 5. (Color online) 'Partial wave cross sections" vs. impact parameter b for the system ^{132}Sn + (α, ^{40}Ca, ^{48}Ca) at 30 MeV/nucleon. In each column are reported the results for the two dipole states, PDR (left frame) and GDR (right frame). In each graph the Coulomb and nuclear contributions are reported and explicitly indicated. Note the different ordinate scales.

energy dependence as the one given by

$$\Gamma = 0.026E^{1.9} \tag{18}$$

according to Ref. [32]. Indeed this energy dependence gives, for the GDR and PDR, approximately the same widths as the previous method used in Ref. [17]. The different contributions from Coulomb and nuclear form factors are separately shown, as well as the total ones. For the latter, we see that by changing the partners of the reaction the balance between PDR and GDR varies appreciably; for the Ca isotopes the PDR peak is higher than the GDR one. In all the three case the GDR peak is dominated by the Coulomb contribution. On the contrary, for the PDR peak, we see that in the α case the nuclear part is dominating while in the Ca isotopes cases the Coulomb and nuclear contributions are equally important. Moreover the previously discussed constructive interference in the form factors for large radii shows up in all cases.

Calculations done so far only include dipole states. Of course the excitation spectra are much richer than those we have studied till now since other multipolarities are present in the region of interest. In particular the low-lying quadrupole and octupole states may have a high probability to be excited at these incident energies. Therefore we have enlarged the channel basis by including in the calculations the states considered in Ref. [17], namely we add, to the already considered dipole states the other states shown in Table II. In the three panels of Fig. 7 we show the energy differential

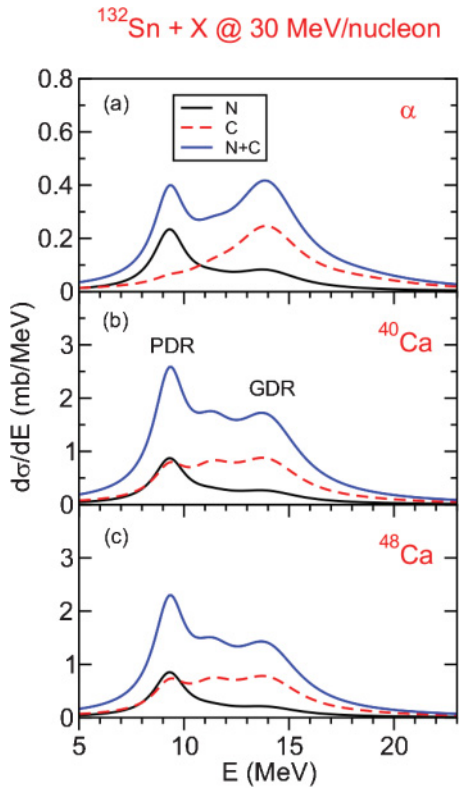

FIG. 6. (Color online) Differential cross sections as function of the excitation energy for the systems ^{132}Sn + α, ^{40}Ca, ^{48}Ca at 30 MeV per nucleon. The Coulomb contribution is shown as a dashed line (red). Of the two solid lines the lower one (black) corresponds to the nuclear contribution while the higher one (blue) represents the total cross section.

cross section for the ^{132}Sn + ^{40}Ca case at 30, 60, and 100 Mev/nucleon incident energy. In the upper (a) and middle (b) panels, the nuclear and Coulomb contributions are shown. In the lower (c) panel, the total cross section shows the interplay between the Coulomb and the nuclear parts of the interaction. We note that the excitation induced by the nuclear part of the interaction is almost independent of the incident energy. On the contrary, in the Coulomb case the variation of the incident energies produces structurally different results. Indeed, by increasing the incident energy the cross section gets bigger in the GDR region while it decreases in the low energy region part. This is due to the well-known adiabatic cut-off effect that governs the transition amplitudes for Coulomb excitation (see for example Ref. [33,34]).

TABLE II. RPA one-phonon basis for the nucleus ^{132}Sn. For each state, energy and percentage of the EWSR are reported.

States	E (MeV)	EWSR %
GMR	16.32	85
2^+_{11}	5.03	11
ISGQR	13.50	77
3^-_{11}	5.93	27

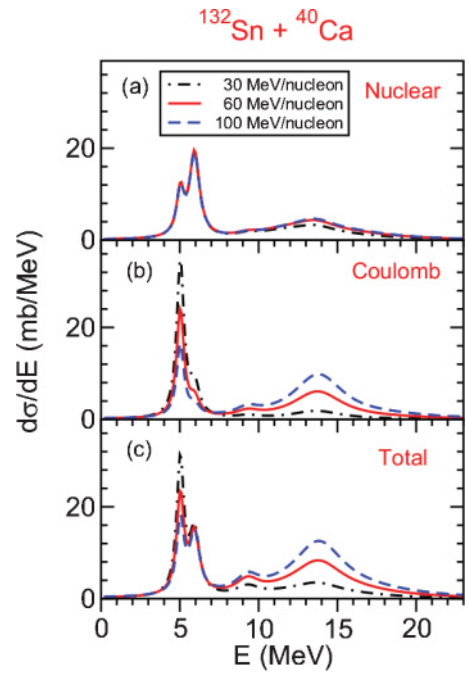

FIG. 7. (Color online) Differential cross sections as function of the excitation energy for the systems ^{132}Sn + ^{40}Ca at three values of incident energies. The nuclear (a) and Coulomb (b) contributions are separately shown.

Nevertheless, it is important to single out the explicit contribution of the dipole states. In Fig. 8 the inelastic cross section for the system ^{132}Sn + ^{40}Ca is reported for three different values of the incident energy. The dipole cross sections are evidenced (shaded areas) against the total ones. We clearly see that the peak around 9.3 MeV excitation energy (the PDR region) contains essentially only dipole contributions, and this is true for all the three considered incident energies.

As far as the other multipole states contributions are concerned, one can have a more complete view of the relative importance of the multipole states and their dependence on the partners of the reaction looking at Fig. 9. There the inelastic cross sections for the three systems ^{132}Sn + (α, ^{40}Ca, ^{48}Ca) at 30 MeV/nucleon are reported and their multipole components are separately shown. The change of the reaction partners modifies the relative intensity of the inelastic cross section especially for the low-lying quadrupole and octupole states. This is due to the different behavior of the nuclear and Coulomb fields in the excitation process.

A global vision of the contribution of different multipolarities can be grasped by looking to Fig. 10 where the nuclear, Coulomb and total inelastic cross section for the states of different multipolarities used in the calculations as function of the incident energy are shown. As one could expect the pure isoscalar states are more excited by the nuclear field (a). The mixed isoscalar and isovector components in the dipole states makes them appreciably excited: the probability for the PDR state is sensibly higher than the GDR one at low incident energies.

The middle panel (b) shows the inelastic cross section produced by the Coulomb field. Note the predominant role

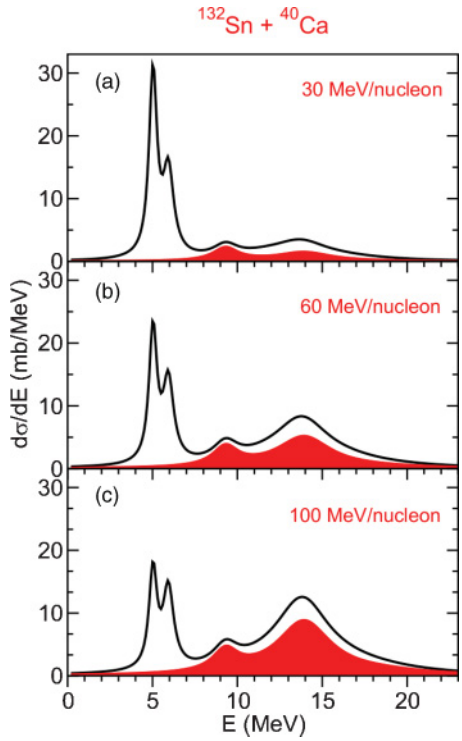

FIG. 8. (Color online) Same as Fig. 7. The solid lines correspond to the total cross section while the shaded (red) area shows the contribution of the dipole states.

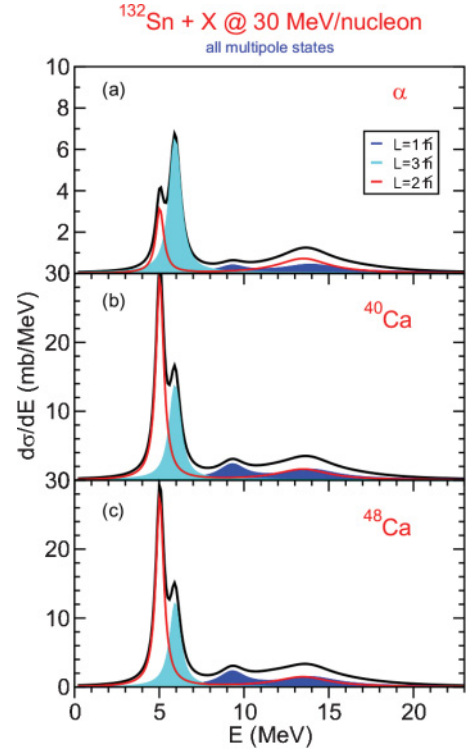

FIG. 9. (Color online) Differential cross sections as function of the excitation energy for the systems ^{132}Sn + (α, ^{40}Ca, ^{48}Ca) at 30 MeV per nucleon. In each frame the multipole contributions are shown. The pale (cyan) shaded area corresponds to the $L = 3$ multipole states while the dark (blue) area is the dipole contributions. The thin (red) and the thick (black) line correspond to the $L = 2$ and total, respectively.

of the GDR as far as the incident energy increases. In minor measure also the GQR behaves in the same fashion. The low-lying states get more excited at low incident energies and then their excitation decreases with the increase of the energy. Both these responses are clearly manifestations of the adiabatic cut-off effect.

The third panel (c) shows the combination of the two contributions described above. The results we have seen until now suggest that the investigation of the PDR state can be better carried out at low incident energy (below 50 MeV/nucleon). In fact, although the PDR cross section is higher at higher incident energy, its peak may be blurred by the strong tail of the giant resonance states. On the other hand the PDR peak should not be masked by the presence of the low-lying quadrupole and octupole states because of their narrow widths.

B. The ^{208}Pb case

As stated in Sec. II, the pygmy states are present also in stable nuclei with neutron excess. The most known case is the one of ^{208}Pb whose transition densities show the same features of the ^{132}Sn as it can be seen in Fig. 2. Therefore one can repeat the same analysis done until now for the ^{132}Sn, with the advantage that one is not limited in the possible range of incident energies as it should be the case for the existing or next future radioactive beams.

In Fig. 11 we present the calculations for inelastic cross section for the system ^{17}O + ^{208}Pb at two incident energies. The calculation have been done by taking into account all the states listed in Table III. The behavior is the same already seen for the ^{132}Sn. The nuclear interaction produces similar results for the two energies (20 and 50 MeV/nucleon) as can be seen in the upper frame (a). The Coulomb excitation favors more the high lying states when the incident energy increases [frame (b)]. The sum of the two contributions, in panel (c), shows clearly the peak of the PDR. In the frame (d) the nuclear and Coulomb contributions are shown together with the total one for a more precise comparison.

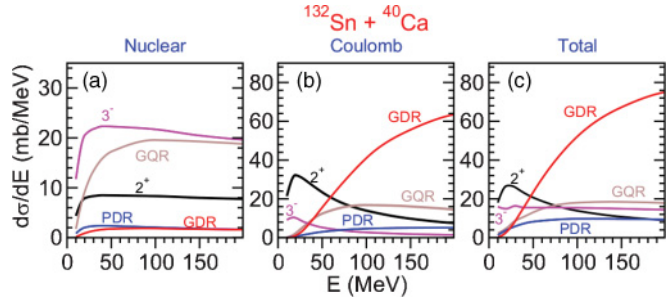

FIG. 10. (Color online) Differential cross sections as function of the incident energy per nucleon for the systems ^{132}Sn + ^{40}Ca for the multipole states used in the calculations. The nuclear (a) and Coulomb (b) contributions, as well as the total one (c), are shown in separate frame.

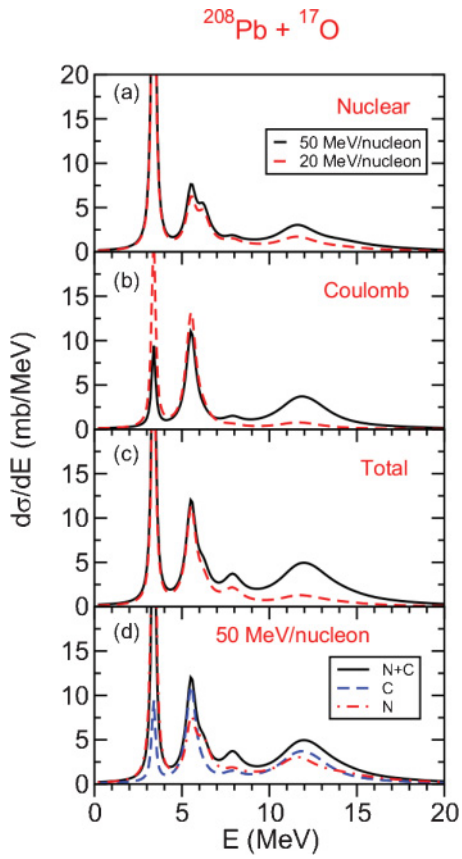

FIG. 11. (Color online) Differential cross sections as function of the excitation energy for the systems ^{208}Pb + ^{17}O for two values of incident energies. The nuclear (a) and Coulomb (b) contributions are separately shown. In the frame (d) the contributions due to the Coulomb and nuclear fields as well as the total one are shown for the higher incident energy case.

The constituents of the inelastic cross section, in terms of multipole states we have take into account, are shown in Fig. 12 for the two incident energies considered here. As in the previously analyzed case, the low-lying states are much more excited but, because of their tiny widths, they do not obscure the presence of the PDR peak which also in this case is due essentially to the excitation of dipole states.

TABLE III. RPA one-phonon basis for the nucleus ^{208}Pb. For each state, energy and percentage of the EWSR are reported.

States	E (MeV)	EWSR %
GMR	14.0	86
PDR	7.9	1.2
GDR	12.4	60
1^-	16.7	17
2^+	5.5	6
ISGQR	11.6	75
3^-_1	3.4	22
3^-_2	6.2	9

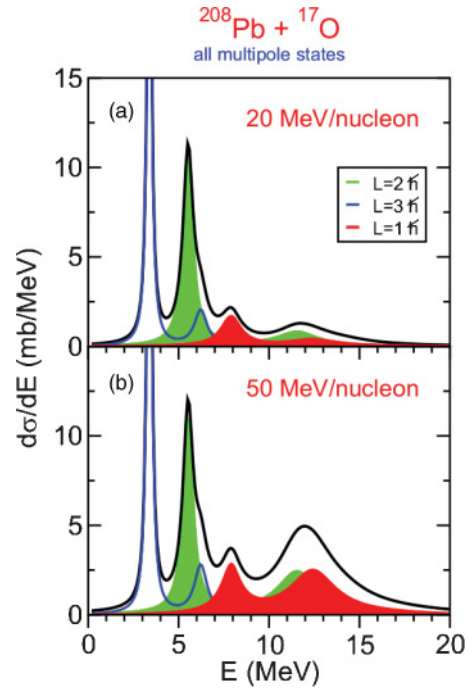

FIG. 12. (Color online) Differential cross sections as function of the excitation energy for the systems ^{208}Pb + ^{16}O for two values of incident energies. The different multipole contributions are separately shown: The pale (green) shaded area corresponds to the $L = 2$ multipole states while the dark (red) area is the dipole contributions. The thin (blue) and the thick (black) line correspond to the $L = 3$ and total, respectively.

V. CONCLUSIONS

In the isovector dipole strength distribution the peak appearing at low energy corresponds to a mode whose isoscalar and isovector components are strongly mixed as it is clearly manifested in their transition densities. This feature allows the possibility to study these so-called pygmy dipole resonance states by using an isoscalar probe in addition to the conventional isovector one. Actually, this has been already done for some semimagical nuclei like the ones studied in Ref. [22]. There, by means of $(\alpha, \alpha'\gamma)$ coincidence method, a splitting of the low-lying dipole bump has been found out. Namely, it was shown that with this method only the low-lying part of the bump is populated while the remnant is excited only by a (γ, γ') experiment. This has been interpreted as due to the properties of the α particle to probe the surface part of the transition density of the nucleus. Hence, only the lower part of the bump seems to show a strong isoscalar component in the peripheral region of the transition density while the states belonging to the high energy region of the bump should have a predominantly isovector transition density. However, all theoretical calculations and analyses done until now within several microscopic many body models agree in considering a transition density with the characteristic features shown in Fig. 2 as a distinctive property of PDR states. Therefore, the higher energy bump should not be interpreted as due to the excitation of states of that nature. This shows in a very clear way that comparing the results obtained by using different

probes one can get valuable information on the structure underlying the peaks observed experimentally.

These PDR states show up when a consistent neutron excess is present in the nucleus; therefore their appearance is more pronounced in nuclei far from the stability line but its presence has been established also for very stable nuclei as ^{208}Pb. Indeed, by studying their transition densities, we have shown that the same feature that characterize the PDR state for the ^{132}Sn are duplicated in the ^{208}Pb case.

We have shown that valuable informations on the nature of the PDR can be obtained by excitation processes involving also the nuclear part of the interaction. The use of different bombarding energies, of different combinations of colliding nuclei involving different mixture of isoscalar/isovector components, together with the mandatory use of microscopically constructed form factors, can provide the clue to reveal the characteristic features of these states. These analyses have been carried out on the ^{132}Sn with different partners of the reaction like ^{4}He, ^{40}Ca, and ^{48}Ca. We found that the excitation induced by the nuclear part of the interaction is almost independent of the incident energy. On the contrary, in the Coulomb case the variation of the incident energies produces structurally different results. This is due to the well-known adiabatic cut-off effect.

We have shown that the relative population of the PDR with respect to the GDR may change by changing the parameters of the reactions. In particular, at low incident energy the excitation probability of the PDR state is sensibly high than the GDR one. Our results then suggest that the investigation of the PDR state can be better carried out at low incident energy (below 50 MeV/nucleon). In fact, at these energies the PDR peak should not be masked by the presence of the low lying quadrupole and octupole states because of their narrow widths. On the contrary, at higher incident energy the PDR cross section is higher but its peak may be blurred by the strong tail of the giant resonance states.

Our conclusion is that the best conditions to reveal the PDR can be achieved at relatively low incident energies (around 30 MeV per nucleon), where the interplay between the Coulomb and nuclear interactions plays a fundamental role in singling out these states. The last example analyzed (^{17}O + ^{208}Pb) has the advantage that, being the partners of the reaction stable nuclei, it is allowed to explore a great variety of incident energies.

ACKNOWLEDGMENTS

One of the authors (M.V.A.) acknowledges the financial support provided by the Spanish Ministerio de Ciencia e Innovación and the European regional development fund (FEDER) under Project Nos. FPA2009-07653 and FIS2008-04189; the Spanish Consolider-Ingenio 2010 Programme CPAN (CSD2007-00042) and Junta de Andalucía under Project Nos. P07-FQM-02894 and FQM160; the bilateral agreement between the Spanish Ministerio de Ciencia e Innovación and the Italian I.N.F.N., AIC10-D-000590.

[1] N. Paar, D. Vretenar, E. Khan, and G. Colò, Rep. Prog. Phys. **70**, 691 (2007), and references therein.
[2] F. Catara and E. G. Lanza, M. A. Nagarajan, and A. Vitturi Nucl. Phys. A **614**, 86 (1997); **624**, 449 (1997).
[3] A. M. Lane, Ann. Phys. (NY) **63**, 171 (1971).
[4] R. Mohen, M. Danos, and L. C. Biedenharn, Phys. Rev. C **3**, 1740 (1971).
[5] H. Steinwedel and J. H. D. Jensen, Z. Naturforsch. **5a**, 413 (1950).
[6] Y. Suzuki, K. Ikeda, and H. Sato, Prog. Theor. Phys. **83**, 180 (1990).
[7] M. Igashira, H. Kitazawa, M. Shimizu, H. Komano, and N. Yamamuro, Nucl. Phys. A **457**, 301 (1986).
[8] P. Van Isacker, M. A. Nagarajan, and D. D. Warner, Phys. Rev. C **45**, R13 (1992).
[9] M. Goldhaber and E. Teller, Phys. Rev. **74**, 1046 (1948).
[10] S. I. Bastrukov, I. V. Molodtsova, D. V. Podgainy, Ş. Mişicu and H.-K. Chang, Phys. Lett. B **664**, 258 (2008).
[11] D. Sarchi and P. F. Bortignon, and G. Coló, Phys. Lett. B **601**, 27 (2004).
[12] D. Vretenar, N. Paar, P. Ring, and G. A. Lalazissis, Nucl. Phys. A **692**, 496 (2001).
[13] N. Paar, T. Nikšić, D. Vretenar, and P. Ring, Phys. Lett. B **606**, 288 (2005).
[14] E. Litvinova, P. Ring, and D. Vretenar, Phys. Lett. B **647**, 111 (2007).
[15] N. Tsoneva, H. Lenske, and Ch. Stoyanov, Phys. Lett. B **586**, 213 (2004); N. Tsoneva and H. Lenske, Phys. Rev. C **77**, 024321 (2008); Mod. Phys. Lett. A **25**, 1779 (2010).
[16] G. Có, V. De Donno, C. Maieron, M. Anguiano, and A. M. Lallena, Phys. Rev. C **80**, 014308 (2009).
[17] E. G. Lanza, F. Catara, D. Gambacurta, M. V. Andrés, and Ph. Chomaz, Phys. Rev. C **79**, 054615 (2009).
[18] P. Adrich *et al.* (LAND-FRS Collaboration), Phys. Rev. Lett. **95**, 132501 (2005); A. Klimkiewicz *et al.* (LAND-FRS Collaboration), Nucl. Phys. A **788**, 145 (2007).
[19] A. Klimkiewicz *et al.*, (LAND Collaboration) Phys. Rev. C **76**, 051603(R) (2007).
[20] O. Wieland *et al.*, Phys. Rev. Lett. **102**, 092502 (2009).
[21] D. Savran *et al.*, Phys. Rev. Lett. **100**, 232501 (2008).
[22] J. Endres *et al.*, Phys. Rev. C **80**, 034302 (2009).
[23] J. Piekarewicz, Phys. Rev. C **73**, 044325 (2006).
[24] A. Carbone, G. Coló, A. Bracco, Li-Gang Cao, P. F. Bortignon, F. Camera, and O. Wieland, Phys. Rev. C **81**, 041301(R) (2010).
[25] N. Van Giai and H. Sagawa, Phys. Lett. B **106**, 379 (1981); Nucl. Phys. A **371**, 1 (1981).
[26] J. A. Christley, E. G. Lanza, S. M. Lenzi, M. A. Nagarajan, and A. Vitturi, J. Phys. G: Nucl. Part. Phys. **25**, 11 (1999).
[27] A. Vitturi, E. G. Lanza, M. V. Andrés, F. Catara, and D. Gambacurta, PRAMANA **75**, 73 (2010); J. Phys.: Conf. Ser. **267**, 012006 (2011); E. G. Lanza, A. Vitturi,

M. V. Andrés, F. Catara, and D. Gambacurta, Nucl. Theory **29**, 162 (2010); A. Georgieva and N. Minkov (eds.), *Twenty Ninth International Workshop on Nuclear Theory* (Heron Press, Sofia, 2010).

[28] G. R. Satchler and W. G. Love, Phys. Rep. **55**, 183 (1979).

[29] G. R. Satchler, *Direct Nuclear Reactions* (Oxford University Press, Oxford, 1983).

[30] G. Bertsch, J. Horysowicz, H. McManus, and W. G. Love, Nucl. Phys. A **284**, 399 (1977).

[31] G. R. Satchler, Nucl. Phys. A **472**, 215 (1987); S. Shlomo, Y. W. Lui, D. H. Youngblood, T. Udagawa, T. Tamura, Phys. Rev. C **36**, 1317 (1987); K. Nakayama and G. Bertsch, Phys. Rev. Lett. **59**, 1053 (1987).

[32] P. Carlos *et al.*, Nucl. Phys. A **219**, 61 (1974).

[33] C. H. Dasso, L. Fortunato, E. G. Lanza, and A. Vitturi, Nucl. Phys. A **724**, 85 (2003).

[34] N. D. Dang, V. K. Au, T. Suzuki, and A. Arima, Phys. Rev. C **63**, 044302 (2001).